ELSEVIER

Archives of Medical Research 43 (2012) 102–111

Archives of Medical Research

ORIGINAL ARTICLE

Osteopontin Upregulation in Atherogenesis Is Associated with Cellular Oxidative Stress Triggered by the Activation of Scavenger Receptors

Azucena E. Jiménez-Corona,[a,*] Salvador Damián-Zamacona,[b,*] Armando Pérez-Torres,[c] Abel Moreno,[a] and Jaime Mas-Oliva[b]

[a]*Instituto de Química,* [b]*Instituto de Fisiología Celular,* [c]*Facultad de Medicina, Universidad Nacional Autónoma de México, Circuito Exterior, C.U. México, D.F., Mexico*

Received for publication December 7, 2011; accepted February 10, 2012 (ARCMED-D-11-00610).

Background. Osteopontin (OPN) is a highly phosphorylated sialoprotein and a prominent component of mineralized extracellular matrices of bones and teeth. Although the structure of OPN has begun to be elucidated, the role of OPN overexpression in tissues distant from the bones and teeth remains poorly understood. In the present study, a rabbit model of hypercholesterolemia was employed to analyze the relationship between the vascular calcification process and OPN overexpression in the neointima of atherosclerotic plaques.

Methods. OPN identification in the aorta of experimental animals fed with a high cholesterol diet was carried out by immunohistochemical procedures and Western blot analysis of tissue homogenates. Transmission electron microscopy was employed to localize target-like extracellular structures of atherosclerotic aortas. The human cell line T/G HA-VSMC was employed in the establishment of a ROS generation model employing the internalization of OxLDL particles.

Results. Using immunohistochemical and Western blot analysis, OPN overexpression was detected in the aortas of rabbits fed a high-cholesterol diet. Results from the ultrastructural analysis of the rabbit neointima through transmission electron microscopy and from the detection of calcium phosphate precipitates by specific histochemical techniques, suggested that OPN may be functionally important as a regulator of vascular calcification. OPN was dramatically overexpressed by vascular smooth muscle cells in the presence of oxidized and acetylated LDL particles bound to scavenger receptors, thereby promoting cytosolic oxidative stress.

Conclusions. This study establishes the *in vivo* role of OPN in the intima of the aorta regulating calcium phosphate precipitate deposition in response to oxidative stress.

Key Words: Osteopontin, Vascular calcification, Atherosclerosis, Oxidized low-density lipoproteins, Scavenger receptor, Oxidative stress.

Introduction

Vascular calcification (VC), defined as the inappropriate deposition of calcium phosphate in cardiovascular structures such as blood vessels and valves, is commonly observed in atherosclerosis and diabetes and is a major concern in patients with chronic kidney disease (1,2). The extracellular matrix (ECM) regulates many physiological and pathological processes (3). In the physiological process of bone development, specific ECM components are produced to create a unique microenvironment that allows the precipitation of calcium and phosphate ions as hydroxyapatite mineral (4). Similarly, in the pathological condition of atherosclerosis, characteristic ECM changes accompany the development of atheroma plaques (5,6).

Vascular calcification is widespread in advanced atherosclerosis and shares many histological features with bone development (7). This and other observations (8) led us to

*These authors contributed equally to the development of this study.

Address reprint requests to: Jaime Mas-Oliva, MD, PhD, Instituto de Fisiología Celular, Universidad Nacional Autónoma de México, Apdo. Postal 70-243, Circuito Exterior C.U., 04510 México, D.F., Mexico; Phone: (+52) (55) 5622-5584; FAX: (+52) (55) 5622-5611; E-mail: jmas@ifc.unam.mx

0188-4409/$ - see front matter.
doi: 10.1016/j.arcmed.2012.03.001

hypothesize that the development of arterial calcification may be regulated in a similar manner to that found during bone formation. This hypothesis is supported by findings in the aged rat heart where endochondral calcification by chondrocytes is associated with types II, X, and pro-I collagen, common proteins in bone formation (9).

Several *in vitro* studies have shown that OPN-deficient smooth muscle cells (SMCs) display an enhanced susceptibility to calcification (10,11). Calcified rheumatic valve neoangiogenesis is associated with vascular endothelial growth factor and OPN upregulation (12). In contrast with fibronectin and type I collagen, which promote the growth of hydroxyapatite (HAP) (7), we previously showed that OPN inhibits hydroxyapatite crystal growth in agarose and silica hydrogels (13).

The binding of OPN to integrin receptors through the highly conserved RGD motif promotes cell adhesion, chemotaxis, and signal transduction in various cell types (14). This combination of ECM effects and intercellular signaling suggests that OPN may also play an important role in tissue repair. Histological studies have demonstrated that lipids are closely associated with the phenomenon of calcification in atherosclerotic lesions. Low-density lipoprotein receptor (RLDL) knockout mice fed a high-fat diet reportedly display hyperlipidemia, VC (15), and a high circulating concentration of modified LDL. As a result, scavenger receptors (SRs) are upregulated, presumably to bind and internalize excess lipid. This process is also associated with increased oxidative stress (16,17).

Scavenger receptors can bind chemically oxidized LDL (oxLDL), methylated bovine serum albumin (M-BSA), *Taenia solium* paramyosin (18), lyinosinic acid, polyguanosinic acid, polysaccharides such as dextran sulfate, fucoidin, lipoteichoic acid, lipopolysaccharide, advanced glycosylation end-products, and amyloid-β peptide (A β), as well as diverse lipid and lipoprotein-based ligands (17,19,20). Chemically oxidized LDLs reportedly increase scavenger receptor class A (SR-A) mRNA and activity levels in smooth muscle cells (SMCs), thereby dramatically increasing the cellular uptake of modified lipoproteins. SR-A gene expression also augments the activity levels of redox-sensitive transcription factors such as AP-1/c-Jun, C/EBPb, and JNK (21), which are important for SMC SR-A upregulation by phorbol esters and reactive oxygen species (ROS) (22).

Scavenger receptor class B (SR-B) recognizes diverse ligands including collagen, fatty acids, anionic phospholipids, thrombospondin, apoptotic cells, native LDL (nLDL), oxLDL, high-density lipoprotein (HDL), and very low-density lipoproteins (VLDLs) (23,24). Scavenger receptor class E (SR-E) is associated with lectin-like oxidized LDL receptor (LOX-1). Originally identified as an endothelial-specific SR, LOX-1 has since been detected in macrophages, SMCs, and platelets (25). A positive feedback loop has been demonstrated between oxLDL uptake and LOX-1 expression in endothelial cells (26).

Together with the modulation of several proteins directly related to oxidative stress, we propose that OPN upregulation in vascular SMCs (VSMCs) and endothelial cells is associated with and mediated by oxidative stress. Through this process, OPN overexpression in the atherosclerotic lesion is markedly associated with the inhibition of calcium deposition in the tissue. These data implicate OPN as a potentially important mediator whose upregulation protects cells from the dystrophic deposition of calcium precipitates of the arterial neointima. This is in contrast with collagen and elastin, which can be considered as inductors of mineral nucleation.

Materials and Methods

Experimental Animal Studies

Control and cholesterol-fed rabbits. Male New Zealand white rabbits (±1.5 kg) were placed in individual stainless steel cages in a room with controlled environmental conditions (temperature 18−22°C, humidity 40−50%, and a 12−12 h artificial light/dark cycle). All animals were acclimatized in the laboratory for 10 days before study initiation. All animal experimentation was performed according to the Declaration of Helsinki and guiding principles in the care and use of experimental animals.

Animals were fed using a well-balanced commercial feed (Harlan 2031) composed of 14.4% total protein, 2.7% lipid, 21.10% cellulose, 43.20% carbohydrates, 8.40% ash, 1.14% calcium, and 0.58% phosphorus. Feed containing cholesterol was prepared by mixing 2% cholesterol (Sigma C-8503) and 10% corn oil with regular feed (27). The diets were used for a period of at least 3 months, with water and food provided ad libitum. Animals were euthanized through an i.v. injection of sodium pentobarbital (70 mg/kg of weight).

Through a median longitudinal incision, the thoracic and peritoneal cavities of the experimental animals were exposed. The complete aorta was dissected from the aortic valve down to the aortic bifurcation. Adipose and connective tissues were removed from the external aortic surface. The aorta was immediately cut longitudinally, and the endothelium was scraped. This tissue was weighed and homogenized in ice-cold lysis buffer (1:20 w/v) (50 mmol Tris-HCl, 0.15 M NaCl, 1% Triton X-100, 0.25% sodium deoxycholate, 1 μg/mL leupeptin, 10 μg/mL aprotinin, 1 mmol PMSF, 0.5 mmol sodium orthovanadate, 1 mmol benzamidine, and 1 mmol EDTA, pH 8.0). An aliquot of each homogenate was used to determine the protein concentration using the bicinchoninic acid method (Pierce, Rockford, IL).

Western Blot Analysis

Proteins contained in the homogenates of control and treated rabbit tissues were characterized using 12% SDS polyacrylamide gels under reducing conditions. Electrophoresed gels

were transferred to PVDF membranes (Bio-Rad Laboratories, Hercules, CA) at 20 V for 90 min. The PVDF membranes were blocked for 1 h at room temperature with 4% BSA in a TBST buffer (0.1 M Tris-HCl, 0.15 M NaCl, and 0.1% Tween-20, pH 7.5). The membranes were washed twice with TBST and incubated overnight at 4°C with the primary mouse antibody anti-OPN developed in goat (1:500; Sigma-07635, Sigma Chemical Co., St. Louis, MO). Membranes were washed four times × 15 min with TBST, incubated with a horseradish peroxidase (HRP)-conjugated anti-goat IgG secondary antibody (1:10000; Santa Cruz Biotechnology, Santa Cruz, CA) at room temperature for 1 h, washed eight times × 15 min with TBST, and developed by enhanced chemiluminescence (ECL) using a Super Signal kit according to the manufacturer's instructions (Pierce). Recombinant mouse OPN (Sigma-02260) was used in all experiments as a positive control.

Immunohistochemical Procedures

Aortas were collected from control and experimental rabbits at necropsy by employing 1-cm-long fragments. Aortas were fixed with 10% buffered neutral formalin for 24 h before being processed for paraffin embedding and sectioning. Aorta sections of 6–8 μm in thickness were mounted on poly-L-lysine-coated slides and stained with hematoxylin and eosin (H&E). The Von Kossa method (for bone and mineral salts of calcium as phosphates, carbonates, and oxalates) and the Alizarin red S procedure (for calcium salts) were also employed according to protocols from the Armed Forces Institute of Pathology (28,29).

Aorta sections were prepared for immunohistochemistry as described (30). Briefly, the sections were mounted on positive-charged slides (Shandon Inc., Pittsburgh, PA), dewaxed with xylene, rehydrated with PBS, and then transferred to plastic Coplin jars containing 0.1 M citrate buffer (pH 6.0) for antigen retrieval. Slides in the Coplin jar were heated in a pressure cooker for 20 min at ~200°C followed by 10 min at ~100°C. The slides were cooled in the jar at room temperature for 15 min and then transferred to 0.15 mol PBS (pH 7.2) until needed.

After antigen retrieval, endogenous peroxidase was inhibited by incubation for 30 min at room temperature with 3% peroxide hydrogen diluted in methanol. Slides were then incubated for 1 h at room temperature in a solution containing PBS, 2% BSA, and 0.01% Triton X-100 to reduce nonspecific background staining. Slides were incubated overnight at 4°C with specific anti-OPN (mouse monoclonal antibody IgG) diluted 1:100 in PBS with 0.1% BSA. After three washes in PBS, slides were incubated in biotinylated anti-mouse secondary antibody for 1 h at room temperature. The avidin-biotin-HRP complex was used and the reaction was developed with 3′3′ diaminobenzidine according to the supplier's instructions (all reagents were from Santa Cruz Biotechnology). Negative controls consisted of tissue sections processed as above, but incubated with normal mouse serum.

Transmission Electron Microscopy

Tissue fragments of 2-mm-thick aorta specimens including the three tunicas were obtained during necropsy and immediately fixed by immersion in 2.5% glutaraldehyde diluted in a 0.2 mol cacodylate buffer (pH 7.4) for 3 h at 4°C. After three washes × 10 min, aorta fragments contained in 0.15 mol cacodylate buffer (pH 7.4) at 4°C were post-fixed with 1% osmium tetroxide in 0.2 mol cacodylate buffer (pH 7.4) for 2 h at 4°C, dehydrated in gradually increasing concentrations of ethanol, and transferred to absolute toluene (two changes × 10 min). Samples were infiltrated at room temperature for 24 h with Araldite 6005-toluene solution (1:1) followed by pure Araldite 6005 (two changes at 60°C) for 2 h. Specimens were embedded in pure Araldite 6005 at 60°C for 36 h. Ultrathin sections obtained with a diamond knife and contrasted with uranyl acetate and lead citrate were examined with a Zeiss EM-109 electron microscope (EM).

Human Cell Line Experiments

Cell culture. The T/G HA-VSMC human cell line developed from the aorta of a healthy female was used (ATCC; CRL-1999). Vascular SMCs were maintained in F12K media containing 0.05 mg/mL ascorbic acid, 0.01 mg/mL insulin, 0.01 mg/mL transferrin, 10 ng/mL sodium selenite, 0.03 mg/mL endothelial cell growth supplement, 10% (final concentration) fetal bovine serum, 10 mmol (final concentration) HEPES, 10 mmol (final concentration) TES, 100 U/mL penicillin, 100 U/mL streptomycin, and 0.01% amphotericin B. Cells were incubated in a humidified environment at 37°C in an atmosphere of 95% air and 5% CO_2.

Preparation of Lipoproteins

The LDL fraction (density: 1.019–1.063 g/mL) was isolated by sequential ultracentrifugation of human plasma (31,32). LDL labeling with 1,1′-dioctadecyl-3,3,3′3′-tetramethylindocarbocyanine perchlorate (DiI) (Molecular Probes, Eugene, OR) and further acetylation (ac) or oxidization were performed as previously described (33,34). The oxidation was terminated by adding EDTA, and the oxLDL were dialyzed against 150 mmol NaCl containing 100 μM EDTA and stored at 4°C (32).

Internalization Assays and Oxidative Stress Measurements

T/G HA-VSMCs were grown for 2–3 weeks prior to the experiment, maintaining cells at ≤10,000 cells/cm^2. Lipoprotein internalization and oxidative stress assays were performed by adding 2.5 μg/mL ox/acLDL and 10 μM

6-carboxy-H_2DCFA for 5 h at 37°C and 5% CO_2 in supplement- and serum-free media (16). Cells were studied employing confocal microscopy (Olympus FluoView 1000) using excitation/emission wavelengths of 488 nm/519 nm for 6-carboxy-H_2DCFA and 543 nm/569 nm for DiI.

Western Blot Analysis

Cells were treated for 5 h with 2.5 μg/mL oxLDL and 2.5 μg/mL acLDL in serum-free media. After performing the internalization assays, the cells were washed twice with PBS and lysed for 45 min at 4°C in lysis buffer (150 mmol NaCl, 10 mmol Tris, pH 7.4, 1% Triton X-100, 0.5% NP40, 1 mmol EDTA, 1 mmol EGTA, 0.2 mmol sodium orthovanadate, 10 mmol benzamidine, 10 μg/mL leupeptin, 10 μg/mL aprotinin, and 250 μmol PMSF). Lysed cells were centrifuged at 1500 g for 10 min at 4°C and the supernatant was recovered. The protein concentration was determined using the Micro-BCA protein assay (Pierce).

Samples (30 μg/lane) were analyzed by SDS−PAGE on 10% gels. The gels were further transferred to a PVDF membrane for antibody treatment (Bio-Rad Laboratories). Membranes were blocked 1 h at 37°C with a blocking TBST buffer (0.1 M Tris-HCl, 0.15 M NaCl, and 0.5% Tween-20, pH 7.6) containing 5% BSA. The membranes were incubated overnight at 4°C with anti-OPN (1:2500), washed four times × 15 min using blocking buffer, incubated with the HRP-conjugated anti-goat IgG secondary antibody (1:10,000) at room temperature for 1h, washed eight times × 15 min with TBST, and treated with an ECL Plus kit according to the supplier's instructions. Recombinant mouse OPN (Sigma-O2260) was used in all experiments as a positive control.

The same membranes were naked and blocked overnight at room temperature with a solution containing 5% fat-free milk and 1% Tween 20 in Tris-buffered saline (TBS), pH 7.6. The membranes were exposed to a monoclonal anti-β actin antibody (1:500) followed by a HRP-conjugated goat anti-mouse IgG secondary antibody (1:5000) for 1 h at 37°C. Membranes were washed with 1% TBS-Tween. HRP activity was detected using the ECL Plus kit according to the supplier's instructions.

Results

Experimental Animal Studies

Detection of OPN in the atherosclerotic plaque. OPN is a major phosphoprotein secreted by osteoblasts (10) and expressed at high levels in a number of transformed cells (35). Due to its posttranslational modifications and its generally acidic nature, OPN presents anomalous migration patterns on SDS-PAGE gels.

The apparent molecular weight of OPN ranges from 31−65 kDa depending on the tissue from which it was extracted and on the detection conditions (36). In human glioma cell lines by Western blot, bands were detected corresponding to a molecular weight of 53, 47, 38 and 31 kDa. Various hormones, cytokines and tumor promoters differentially regulate the two prominent forms of OPN that migrate at 55 and 44 kDa. Several previous studies have shown that multiple forms of OPN are generated by differences in posttranslational modification such as phosphorylation, glycosylation and sulfation. Other studies have shown that the 44 kDa species OPN is a glycosylated and phosphorylated form of the nonphosphorylated 32 kDa protein, with phosphate groups associated with 12 serines and one threonine residue (37,38).

Therefore, the 31-kDa band detected in the present study may be protein unmodified or degraded or posttranslationally modified products of larger species or alternatively spliced species (Figure 1).

In the case of recombinant OPN (Sigma-O2260), the protein migrates as a single band at 65 kDa on reducing SDS-PAGE (39). Under the experimental conditions used in this study, endothelial tissue recovered from normal aortas obtained from control animals did not show the presence of OPN, whereas tissues obtained from animals subjected to a cholesterol-supplemented diet showed an important reaction for this protein (65 kDa) (Figure 1).

Histopathology. After 3 months of treatment, all animals on the cholesterol-supplemented diet developed atherosclerosis with its characteristic pattern and histopathological features (Figure 2). In the thoracic and abdominal

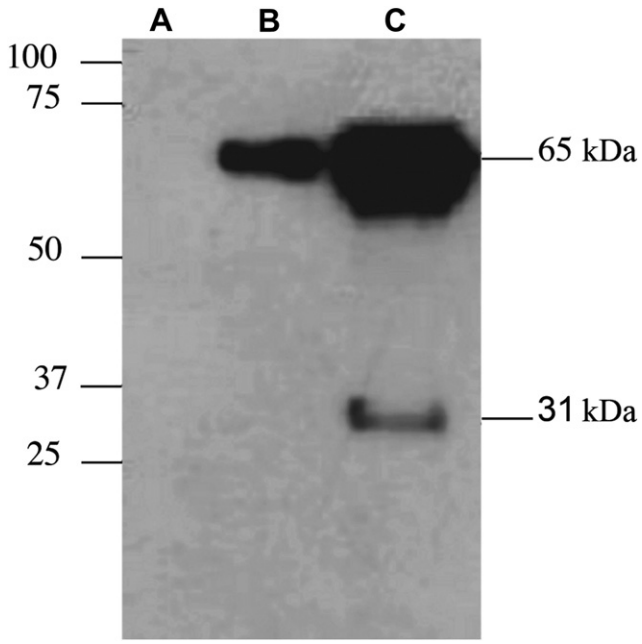

Figure 1. Osteopontin (OPN) identification by Western blot analysis. (A) Protein preparation from a control aorta. (B) Control recombinant OPN. (C) Aorta obtained from an animal fed a high-cholesterol diet. Representative experiment in a series of four independent assays.

aorta specimens, the intima was thickened by up to 50% of the normal lumen perimeter. The subendothelial neointima layer was composed of spindle-shaped cells, probably corresponding to SMCs and/or fibroblasts and aggregated foam cells, all embedded in connective tissue (Figure 2A). These features were also observed in slender atheromatous lesions within the subendothelial layer of the aortas with an apparently normal structure for the tunica intima. The innermost elastic lamina appeared disrupted at sites where atherosclerotic lesions had a well-developed neointima and appeared conserved at sites of moderate atheromatous lesions.

Clusters of basophilic granules were identified in proximity to the tunica media, near the disrupted innermost elastic lamina. Similar single granules were also observed dispersed in the neointima (Figure 2A) surrounded by foam cells and stellated cells showing a vacuolated cytoplasm. Many basophilic granules showed a target-like structure with a rather light and eosinophilic center (Figure 2D).

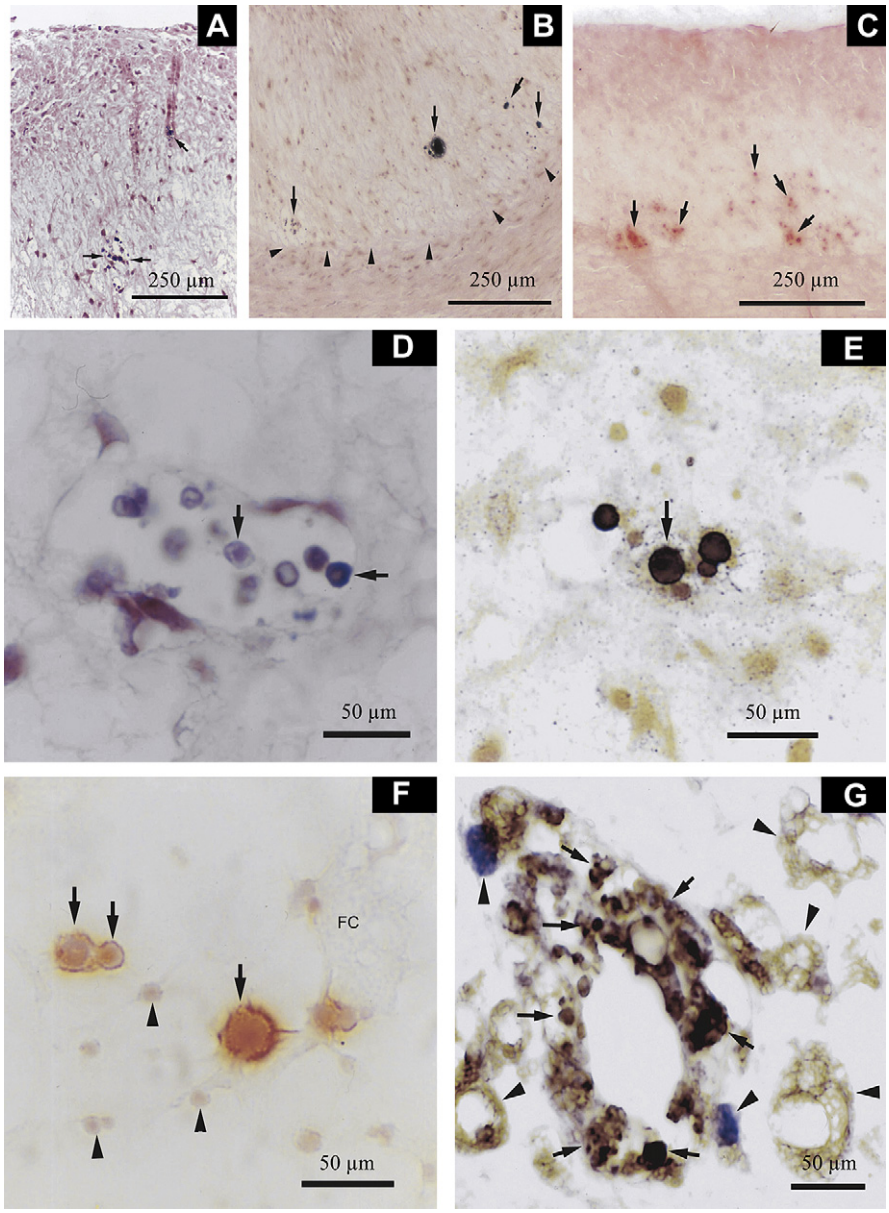

Figure 2. Atherosclerotic lesions of aortas from rabbits fed a high-cholesterol diet. (A,D; arrows) The neointima displayed the characteristic features of an atheroma plaque, with the presence of basophilic granules. (B,E) Aortas were also stained with the Von Kossa method at the boundary between the neointima and the tunica media (B, arrowheads). Alternative calcium staining with Alizarin red S confirmed that these target-like structures (C,F) surrounded by foam cells (F, FC) were associated with calcium mineralization. Immunohistochemical staining demonstrated a close association between extracellular (G, arrows) and cellular (G, foam cells marked with arrowheads) OPN and the presence of calcium deposits. Bars: A–C, 250 µm; D–G, 50 µm. Representative experiment in a series of two independent assays performed with two control and two animals fed a high-cholesterol diet.

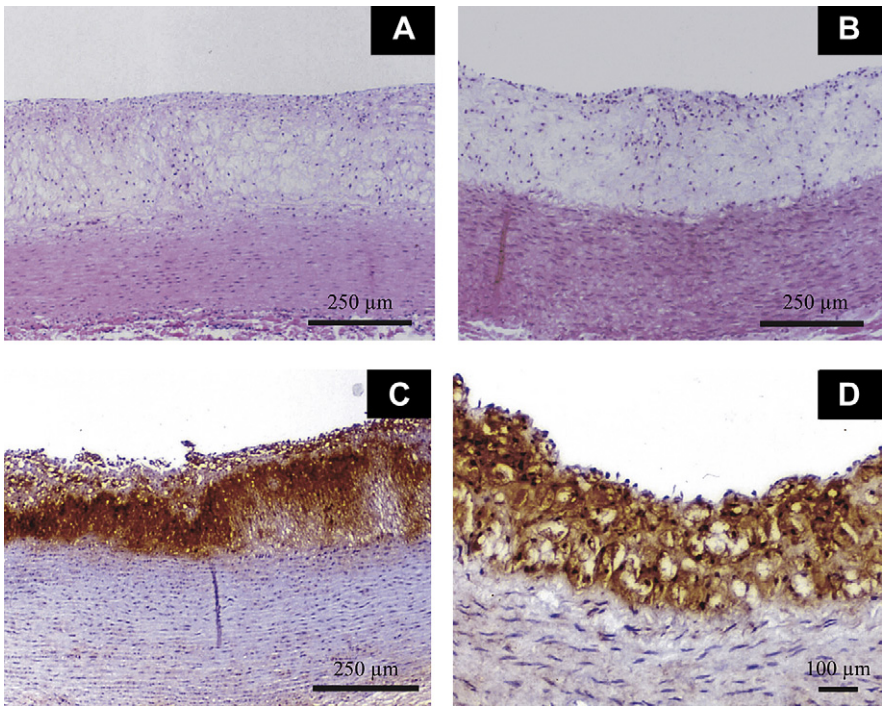

Figure 3. Immunohistochemistry for OPN in thoracic (A,C) and abdominal (B,D) aortas from experimental atherosclerotic rabbits. (C,D) Aortas show atheroma plaques in both the thoracic and abdominal regions, and the overexpression of OPN at the neointima. (D) The tunica media of SMCs also weakly expresses OPN. Bars: A–C, 250 µm; D, 100 µm. Representative experiment in a series of two independent assays performed with two control and two animals fed a high cholesterol diet.

Calcium staining. Tissue sections from atherosclerotic thoracic and abdominal aortas stained by the Von Kossa method showed black granules that appeared as isolated dots or as clusters along and near the internal elastic lamina as well as at the neointima (Figures 2B,E). The diameter of the smaller granules of metallic silver, which corresponded to deposits of calcium salts, ranged from 1–2 µm. The diameter of the larger granules measured ~10 µm. Few granules had a diameter close to 30 µm. Most of the Von Kossa-positive granules displayed a target-like structure appearance close to the basophilic granules stained with H&E (Figure 2E). Both granule types were located in similar places at the neointima. Specimens stained with Alizarin red S were similar to those stained by the Von Kossa method, except that the Alizarin Red S-calcium complex was formed via a chelation process that yielded orange-colored granules (Figures 2C,F).

OPN immunohistochemistry. According to immunohistochemical analysis, rabbits fed a cholesterol-supplemented diet displayed a high expression of OPN in the neointima of aortic atherosclerotic plaques. Immunoreaction was less apparent at the tunica media and in scattered cells of the tunica adventitia (Figure 3). The neointimal OPN staining was localized mainly at the cytoplasm of three cell types: endothelial cells, macrophage-derived or rounded foam cells, and fusiform cells similar to SMCs and fibroblasts. Other than staining for OPN, the most extensive extracellular staining was observed surrounding spherical structures morphologically compatible to basophilic granules. These structures were positive for both the Von Kossa and Alizarin red stains (Figure 2G). Aortas from control animals showed a faint level of OPN expression, mostly located in the endothelial cells and SMCs of the tunica media (data not shown).

Ultrastructural analysis of atherosclerotic aortas. Compared to normal aortas, the analysis of atherosclerotic aortas by electron microscopy revealed target-like extracellular structures with concentric electron-dense and -lucent rings located at the boundary between the neointima and the tunica media (Figure 4). This finding was consistent with other studies in which these structures were associated with VC (35). Most of these structures were observed in proximity to the collagen fibrils. They were also found near a relatively amorphous material surrounded by microfibrils, which corresponded to the innermost of the many elastic layers present in the tunica media of the aortic wall.

Human Cell Line Experiments

Oxidative stress induction and detection of OPN in T/G HA VSMCs. The lesion type described above is associated

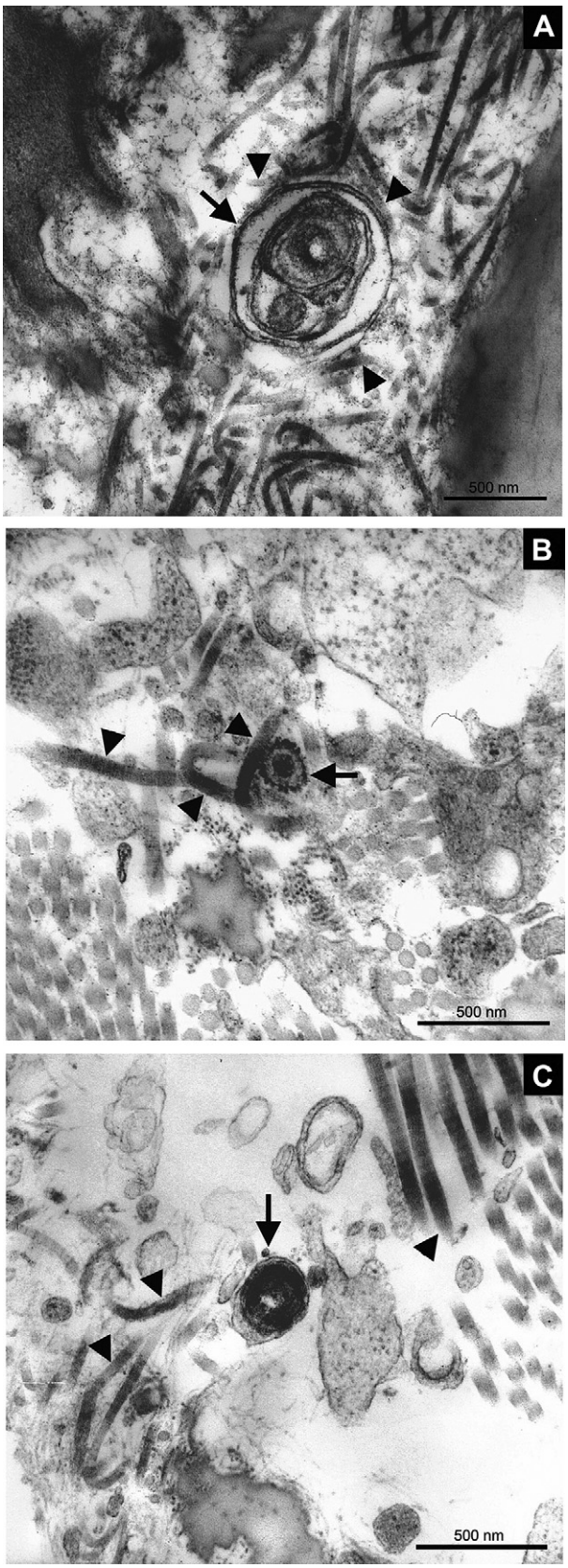

Figure 4. Transmission electron micrographs of atherosclerotic rabbit aortas at the boundary between the neointima and the tunica media. Note the presence of target-like extracellular structures (arrows) in proximity with collagen fibrils (arrowheads) near an amorphous material surrounded by microfibrils associated with the elastic lamellas. (A,B) Samples taken from the thoracic aorta. (C) Sample taken from the abdominal aorta. Bars correspond to 0.5 μm. Representative experiment in a series of two independent assays performed with two control and two animals fed a high-cholesterol diet.

with modified lipoproteins and their internalization in endothelial cells, SMCs, and macrophages which, in turn, causes a state of oxidative stress (21,22,25). Therefore, we explored the potential relationship between this inductive metabolic state and overexpression of OPN observed in the aortas of cholesterol-fed experimental animals.

To verify that the exposure of VSMCs to oxLDL caused oxidative stress, we conducted 5 h internalization tests of oxLDL labeled with DiI (DiI-oxLDL) and DiI-acLDL. DiI-oxLDL and DiI-acLDL were simultaneously incubated with 6-carboxy-H2DCFA, a label that shows fluorescence by reacting with free radicals including ROS. The internalization of oxLDL occurred concomitant with ROS formation, as evidenced by ROS colocalization with DiI-labeled internalized oxLDLs (Figure 5).

To demonstrate whether the observed state of oxidative stress produced by ox/acLDL endocytosis altered OPN synthesis in the VSMCs, internalization experiments were performed that utilized the ubiquitous expression of SR-A and SR-B in VSMCs. Western blot analysis revealed that VSMCs treated with oxLDL and acLDL, but not those unexposed to chemically treated lipoproteins, expressed OPN (Figure 6). The differences in antibody reactivity observed between commercial OPN (used as a control) and OPN expressed by our cultured cells were most likely related to posttranslational processing and/or the degree of protein degradation associated with the process of apoptosis. We previously showed that apoptosis can be triggered through the internalization of modified lipoproteins in the presence of oxidative stress (17).

Our results strongly support the hypothesis that oxidative stress triggers the overexpression of OPN, a molecule that helps to modulate calcium precipitation in the atherosclerotic plaque.

Discussion

Osteopontin (OPN) is expressed in proliferating and migratory vascular cells and is associated with neointima formation. OPN is also directly associated with atherosclerotic lesions, a finding that correlates well with the observed increased SMC proliferation and production of matrix metalloproteases (40,41). Calcified nodules first form in regions of lipid deposition, particularly those involved with oxidized lipids (42). In response to oxidized cholesterol, transforming growth factor-β_1, bone morphogenetic protein

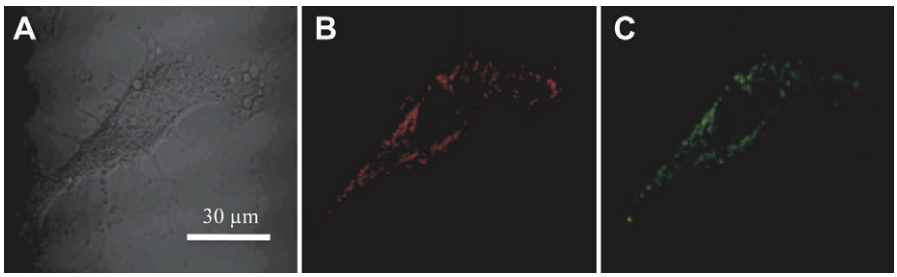

Figure 5. Internalization of oxidized low-density lipoprotein (oxLDL) and generation of reactive oxygen species (ROS) in vascular smooth muscle cells (VSMCs). T/G HA-VSMCs incubated during culture with DiI-oxLDL (to follow lipoprotein internalization) and 6-carboxy-H_2DCFA (oxidative stress marker). (A) Phase contrast image showing T/G HA-VSMCs. (B) OxLDL internalization. (C) Oxidative stress marker associated with ROS generation. The excitation/emission wavelengths were 448 nm/519 nm for 6-carboxy-H_2DCFA and 543 nm/569 nm for DiI. Bar =30 µm. Representative experiment in a series of four independent assays.

(BMP)-2 (43), and RANKL (44), an increase in the rate of calcified nodule formation and the development of osteoblast markers has been observed. Bone tissue calcification is initiated in small vesicular structures containing HAP crystals, designated as matrix vesicles. Interestingly, matrix vesicles have also been found in atherosclerotic lesions (45). These observations are supported by our present findings showing that OPN is immunodetected in SMCs and foam cells in atherosclerotic lesions associated with calcium deposits.

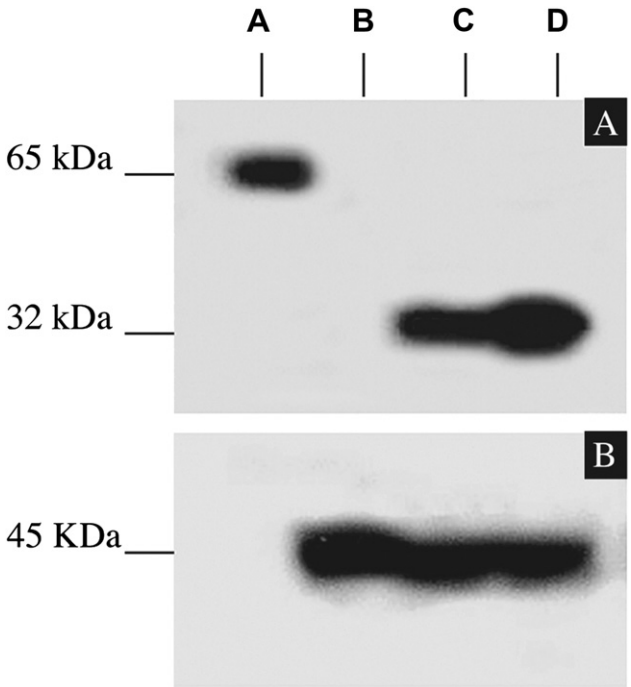

Figure 6. OPN identification by Western blot analysis. (Lane A) Control recombinant OPN; (Lane B) VSMCs incubated for 5 h in the absence of chemically modified lipoproteins and serum-free media; (Lanes C and D) VSMCs after internalization of ox-LDL (C) and acLDL (D). (A) Immunoblots developed for OPN and (B) β-actin as loading control. Representative experiment in a series of four independent assays.

Human VSMCs *in vitro* and *in vivo* display a phenotypic change that is often associated with their ability to acquire characteristics of a diverse range of mesenchymal lineages, including osteoblastic, chondrocytic, and adipocytic (46). *In vitro*, modified lipoproteins stimulate VSMC calcification and promote protein gene expression related to osteogenic differentiation (47,48). Vascular calcification may reportedly occur through the induction of osteogenesis and the establishment of an osteochondrogenic phenotype regulated by BMP. BMP-2 can promote phosphate uptake and the calcification of human VSMCs (49). Once the osteogenic phenotype is induced, cells gain a distinctive molecular fingerprint marked by specific transcription factors including Msx2. Msx2 promotes osteogenesis and suppresses the adipogenic differentiation of multipotent mesenchymal progenitors in a hyperlipidemic diabetic mouse model for VC. Myofibroblasts can be diverted to an osteogenic lineage through BMP2-Msx2 signaling, which can contribute to VC (50).

OPN is overexpressed after cardiac damage by mechanical trauma or oxidation agents and, therefore, is proposed as important in the reduction of inflammation and tissue remodeling (51,52). OPN is thought to regulate the processes of tissue inflammation and tissue repair, particularly in responses associated with T cells, macrophages, and fibroblasts. This is supported by the finding that OPN expression during the process of dystrophic calcification correlates well with the tissue infiltration of T cells and macrophages (53). Thus, depending on the particular cellular conditions, OPN may influence pro- or anti-inflammatory effects *in vitro* (e.g., by increasing or decreasing the IL-12 or IL-10 level, respectively (54). In this respect, rheumatic valve calcification is not a random passive process, but a regulated inflammatory cellular process associated with the expression of osteoblast markers and neoangiogenesis (12).

Because inflammation is directly correlated with a state of oxidative stress, our experiments suggest that an increased ROS level within the cell may modulate OPN gene expression. ROS can be considered as secondary messengers in the transduction of signals dependent on tyrosine phosphorylation, calcium signaling, or the specific expression of

specific genes (21,55–57). In the case of oxLDL, a calcium signaling cascade is stimulated that increases the cytoplasmic concentration of free calcium (21).

Expression of SR-A may depend on the cytoplasmic calcium concentration. This is indicated by the finding that SR-A is inhibited or potentiated by the specific blockage of plasma membrane calcium channels or the use of calcium ionophores such as A23187, respectively (21). Under conditions that predispose VSMCs to a state of oxidative stress, increased SR-A expression is associated with the activation of AP1/c-Jun (21,22). Phosphorylated AP-1 binds to specific sites in the promoter of TGF-ß, laminin, collagen 1, angiotensin II and OPN, all of which are associated with cellular proliferation, differentiation, and response to ROS (58).

Oxidized LDL not only acts in the transformation of macrophages into foam cells, but also induces the aberrant production of cytokines important in atherosclerotic development. Among the pro-inflammatory cytokines expressed, interleukin 1β (IL-1) and tumor necrosis factor (TNF-α) are both induced by several SR-A ligands (59). Moreover, the activity of SR-A in VSMCs can be modulated by phorbol esters and by the combination of H_2O_2 and vanadate (60). In this respect, we have found that an induced state of oxidative stress directly affects the posttranslational events of SR-A in cultured cells, without altering the transcriptional processing of the receptor (16,17) . Employing an extensive computational approach, Partridge et al. recently identified sets of genes whose transcriptional states were predictive of OPN gene expression (61). These sets included several genes that were associated with redox-regulated transcription (21,61).

Our findings show that OPN overexpression is associated with the presence of extracellular oxLDL and acLDL which, in turn, trigger a state of oxidative stress and possibly initiate apoptosis when bound and internalized by SR-A. We propose OPN as a key molecule associated with and regulated by oxidative stress. We also suggest that ROS promote the overexpression of OPN, which is strikingly associated with the activation of scavenger receptors in cells associated with atherosclerotic plaques. Because redox-regulated transcription is frequently studied in association with changes in gene expression, our laboratory is actively seeking the potential source of ROS after the activation of scavenger receptors and the relationship of this ROS source with OPN transcription factor response elements.

In summary, this study establishes a direct connection between OPN overexpression, which is mediated by the internalization of modified lipoproteins through their binding to scavenger receptors and the concomitant establishment of an oxidative stress state. Together with our previous reports, this study supports the hypothesis that cellular OPN is associated with atherosclerotic plaques and may serve as a buffering molecule in the process of tissue calcification.

Acknowledgments

This study was supported by grants from Consejo Nacional de Ciencia y Tecnología (CONACYT) (No. 47333/A-1 to JM-O and No. 82888 to AM) and the Dirección General de Asuntos del Personal Académico, Universidad Nacional Autónoma de México (DGAPA-UNAM) (No. IN228607/18 to JM-O). We also thank Blanca Delgado-Coello, Martha Ustarroz, Edith Fernández, and Héctor Malagón for their technical assistance and Dr. José Gutierrez Salinas for plasma samples.

References

1. London GM, Guerin AP, Marchais SJ, et al. Arterial media calcification in end-stage renal disease: impact on all-cause and cardiovascular mortality. Nephrol Dial Transplant 2003;18:1731–1740.
2. Wayhs R, Zelinger A, Raggi P. High coronary artery calcium scores pose an extremely elevated risk for hard events. J Am Coll Cardiol 2002;39:225–230.
3. Adams JC, Watt FM. Regulation of development and differentiation by the extracellular matrix. Development 1993;117:1183–1198.
4. Daniels K, Solursh M. Modulation of chondrogenesis by the cytoskeleton and extracellular matrix. J Cell Sci 1991;100:249–254.
5. Canfield AE, Farrington C, Dziobon MD, et al. The involvement of matrix glycoproteins in vascular calcification and fibrosis: an immunohistochemical study. J Pathol 2002;196:228–234.
6. Rekhter MD. Collagen synthesis in atherosclerosis: too much and not enough. Cardiovasc Res 1999;41:376–384.
7. Watson KE, Parhami F, Shin V, et al. Fibronectin and collagen I matrixes promote calcification of vascular cells in vitro, whereas collagen IV matrix is inhibitory. Arterioscler Thromb Vasc Biol 1998;18:1964–1971.
8. Mohler ER 3rd, Gannon F, Reynolds C, et al. Bone formation and inflammation in cardiac valves. Circulation 2001;103:1522–1528.
9. Fitzpatrick LA, Turner RT, Ritman ER. Endochondral bone formation in the heart: a possible mechanism of coronary calcification. Endocrinology 2003;144:2214–2219.
10. Giachelli CM, Bae N, Almeida M, et al. Osteopontin is elevated during neointima formation in rat arteries and is a novel component of human atherosclerotic plaques. J Clin Invest 1993;92:1686–1696.
11. Speer MY, Chien YC, Quan M, et al. Smooth muscle cells deficient in osteopontin have enhanced susceptibility to calcification in vitro. Cardiovasc Res 2005;66:324–333.
12. Rajamannan NM, Nealis TB, Subramaniam M, et al. Calcified rheumatic valve neoangiogenesis is associated with vascular endothelial growth factor expression and osteoblast-like bone formation. Circulation 2005;111:3296–3301.
13. Jimenez-Corona AE, Perez-Torres A, Mas-Oliva J, et al. Effect of osteopontin, chondroitin sulfates (B, C), and human serum albumin on the crystallization behavior of hydroxyapatite in agarose and silica hydrogels. Crystal Growth Design 2008;8:1335–1339.
14. Liaw L, Almeida M, Hart CE, et al. Osteopontin promotes vascular cell adhesion and spreading and is chemotactic for smooth muscle cells in vitro. Circ Res 1994;74:214–224.
15. Towler DA, Bidder M, Latifi T, et al. Diet-induced diabetes activates an osteogenic gene regulatory program in the aortas of low density lipoprotein receptor-deficient mice. J Biol Chem 1998;273:30427–30434.
16. Aguilar-Gaytan R, Mas-Oliva J. Oxidative stress impairs endocytosis of the scavenger receptor class A. Biochem Biophys Res Commun 2003;305:510–517.
17. Manzano-Leon N, Delgado-Coello B, Mas-Oliva J, et al. Beta-adaptin: key molecule for microglial scavenger receptor function under oxidative stress. Biochem Biophys Res Commun 2006;351:588–594.
18. Guaderrama-Diaz M, Solis CF, Velasco-Loyden G, et al. Control of scavenger receptor-mediated endocytosis by novel ligands of different length. Mol Cell Biochem 2005;271:123–132.

19. de Winther MP, van Dijk KW, Havekes LM, et al. Macrophage scavenger receptor class A: a multifunctional receptor in atherosclerosis. Arterioscler Thromb Vasc Biol 2000;20:290−297.
20. Paresce DM, Ghosh RN, Maxfield FR. Microglial cells internalize aggregates of the Alzheimer's disease amyloid beta-protein via a scavenger receptor. Neuron 1996;17:553−565.
21. Mietus-Snyder M, Gowri MS, Pitas RE. Class A scavenger receptor up-regulation in smooth muscle cells by oxidized low density lipoprotein. Enhancement by calcium flux and concurrent cyclooxygenase-2 up-regulation. J Biol Chem 2000;275:17661−17670.
22. Mietus-Snyder M, Glass CK, Pitas RE. Transcriptional activation of scavenger receptor expression in human smooth muscle cells requires AP-1/c-Jun and C/EBPbeta: both AP-1 binding and JNK activation are induced by phorbol esters and oxidative stress. Arterioscler Thromb Vasc Biol 1998;18:1440−1449.
23. Calvo D, Gomez-Coronado D, Suarez Y, et al. Human CD36 is a high affinity receptor for the native lipoproteins HDL, LDL, and VLDL. J Lipid Res 1998;39:777−788.
24. Rigotti A, Acton SL, Krieger M. The class B scavenger receptors SR-BI and CD36 are receptors for anionic phospholipids. J Biol Chem 1995;270:16221−16224.
25. Chen M, Masaki T, Sawamura T. LOX-1, the receptor for oxidized low-density lipoprotein identified from endothelial cells: implications in endothelial dysfunction and atherosclerosis. Pharmacol Ther 2002; 95:89−100.
26. Aoyama T, Fujiwara H, Masaki T, et al. Induction of lectin-like oxidized LDL receptor by oxidized LDL and lysophosphatidylcholine in cultured endothelial cells. J Mol Cell Cardiol 1999;31:2101−2114.
27. Kritchevsky D, Tepper SA, Langan J. Cholesterol vehicle in experimental atherosclerosis. IV. Influence of heated fat and fatty acids. J Atheroscler Res 1962;2:15−22.
28. Allen TC. Hematoxylin and eosin. In: Prophet EB, Millis B, Arrington JB, Sobin LH, eds. Laboratory Methods in Histotechnology. Washington, DC: Armed Forces Institute of Pathology; 1992. p. 53.
29. Johnson FB. Pigments and minerals. In: Prophet EB, Millis B, Arrington JB, Sobin LH, eds. Laboratory Methods in Histotechnology. Washington, DC: Armed Forces Institute of Pathology; 1992. pp. 197−198.
30. Shi SR, Chaiwun B, Young L, et al. Antigen retrieval technique utilizing citrate buffer or urea solution for immunohistochemical demonstration of androgen receptor in formalin-fixed paraffin sections. J Histochem Cytochem 1993;41:1599−1604.
31. Sawamura T, Kume N, Aoyama T, et al. An endothelial receptor for oxidized low-density lipoprotein. Nature 1997;386:73−77.
32. Dejager S, Mietus-Snyder M, Friera A, et al. Dominant negative mutations of the scavenger receptor. Native receptor inactivation by expression of truncated variants. J Clin Invest 1993;92:894−902.
33. Pitas RE, Innerarity TL, Weinstein JN, et al. Acetoacetylated lipoproteins used to distinguish fibroblasts from macrophages in vitro by fluorescence microscopy. Arteriosclerosis 1981;1:177−185.
34. Innerarity TL, Pitas RE, Mahley RW. Lipoprotein-receptor interactions. Methods Enzymol 1986;129:542−565.
35. Senger DR, Asch BB, Smith BD, et al. A secreted phosphoprotein marker for neoplastic transformation of both epithelial and fibroblastic cells. Nature 1983;302:714−715.
36. Rittling SR, Feng F. Detection of mouse osteopontin by western blotting. Biochem Biophys Res Commun 1998;250:287−292.
37. Kasugai S, Zhang Q, Overall CM, et al. Differential regulation of the 55 and 44 kDa forms of secreted phosphoprotein 1 (OPN, osteopontin) in normal and transformed rat bone cells by osteotropic hormones, growth factors and a tumor promoter. Bone Mineral 1991;13:235−250.
38. Saitoh Y, Kuratsu J, Takeshima H, et al. Expression of osteopontin in human glioma. Its correlation with the malignancy. Lab Invest 1995;72:55−63.
39. Miyazaki Y, Setoguchi M, Yoshida S, et al. The mouse osteopontin gene. Expression in monocytic lineages and complete nucleotide sequence. J Biol Chem 1990;265:14432−14438.
40. Castellano G, Malaponte G, Mazzarino MC, et al. Activation of the osteopontin/matrix metalloproteinase-9 pathway correlates with prostate cancer progression. Clin Cancer Res 2008;14:7470−7480.
41. Isoda K, Nishikawa K, Kamezawa Y, et al. Osteopontin plays an important role in the development of medial thickening and neointimal formation. Circ Res 2002;91:77−82.
42. Olsson M, Thyberg J, Nilsson J. Presence of oxidized low density lipoprotein in nonrheumatic stenotic aortic valves. Arterioscler Thromb Vasc Biol 1999;19:1218−1222.
43. Mohler ER 3rd, Chawla MK, Chang AW, et al. Identification and characterization of calcifying valve cells from human and canine aortic valves. J Heart Valve Dis 1999;8:254−260.
44. Kaden JJ, Bickelhaupt S, Grobholz R, et al. Receptor activator of nuclear factor kappaB ligand and osteoprotegerin regulate aortic valve calcification. J Mol Cell Cardiol 2004;36:57−66.
45. Hsu HH, Camacho NC, Tawfik O, et al. Induction of calcification in rabbit aortas by high cholesterol diets: roles of calcifiable vesicles in dystrophic calcification. Atherosclerosis 2002;161:85−94.
46. Tyson KL, Reynolds JL, McNair R, et al. Osteo/chondrocytic transcription factors and their target genes exhibit distinct patterns of expression in human arterial calcification. Arterioscler Thromb Vasc Biol 2003;23:489−494.
47. Parhami F, Basseri B, Hwang J, et al. High-density lipoprotein regulates calcification of vascular cells. Circ Res 2002;91:570−576.
48. Proudfoot D, Davies JD, Skepper JN, et al. Acetylated low-density lipoprotein stimulates human vascular smooth muscle cell calcification by promoting osteoblastic differentiation and inhibiting phagocytosis. Circulation 2002;106:3044−3050.
49. Li X, Yang HY, Giachelli CM. BMP-2 promotes phosphate uptake, phenotypic modulation, and calcification of human vascular smooth muscle cells. Atherosclerosis 2008;199:271−277.
50. Cheng SL, Shao JS, Charlton-Kachigian N, et al. MSX2 promotes osteogenesis and suppresses adipogenic differentiation of multipotent mesenchymal progenitors. J Biol Chem 2003;278:45969−45977.
51. Kossmehl P, Schonberger J, Shakibaei M, et al. Increase of fibronectin and osteopontin in porcine hearts following ischemia and reperfusion. J Mol Med 2005;83:626−637.
52. Okamoto H. Osteopontin and cardiovascular system. Mol Cell Biochem 2007;300:1−7.
53. Giachelli CM, Lombardi D, Johnson RJ, et al. Evidence for a role of osteopontin in macrophage infiltration in response to pathological stimuli in vivo. Am J Pathol 1998;152:353−358.
54. Ashkar S, Weber GF, Panoutsakopoulou V, et al. Eta-1 (osteopontin): an early component of type-1 (cell-mediated) immunity. Science 2000;287: 860−864.
55. Doan TN, Gentry DL, Taylor AA, et al. Hydrogen peroxide activates agonist-sensitive Ca^{2+}-flux pathways in canine venous endothelial cells. Biochem J 1994;297:209−215.
56. Finkel T. Oxygen radicals and signaling. Curr Opin Cell Biol 1998;10: 248−253.
57. Suzuki YJ, Ford GD. Superoxide stimulates IP3-induced Ca^{2+} release from vascular smooth muscle sarcoplasmic reticulum. Am J Physiol 1992;262:H114−H116.
58. Wang KX, Denhardt DT. Osteopontin: role in immune regulation and stress responses. Cytokine Growth Factor Rev 2008;19:333−345.
59. Hsu HY, Chiu SL, Wen MH, et al. Ligands of macrophage scavenger receptor induce cytokine expression via differential modulation of protein kinase signaling pathways. J Biol Chem 2001;276: 28719−28730.
60. Mietus-Snyder M, Friera A, Glass CK, et al. Regulation of scavenger receptor expression in smooth muscle cells by protein kinase C: a role for oxidative stress. Arterioscler Thromb Vasc Biol 1997;17: 969−978.
61. Partridge CR, He Q, Brun M, et al. Genetic networks of cooperative redox regulation of osteopontin. Matrix Biol 2008;27:462−474.